

## Coupling of 3D Analytical Calculation and PSO for the Identification of Magnet Parameters used in Magnetic Separation

M. Ouili<sup>1</sup>, R. Mehasni<sup>1</sup>, M. Feliachi<sup>2</sup>, H. Allag<sup>3</sup>, H. R. E. H. Boucekara<sup>4</sup>,  
G. Berthiau<sup>2</sup>, and M. E. H. Latreche<sup>1</sup>

<sup>1</sup>Laboratoire d'électrotechnique de Constantine (LEC)  
Université des frères Mentouri Constantine 1, Route Ain Elbey, 25000 Constantine, Algérie  
mehdi.ouili@lec-umc.org, mehasni@yahoo.fr, meh\_latreche@univ-constantine2.dz

<sup>2</sup>Laboratoire IREENA  
Université de Nantes, CRTT, BP 406, Boulevard de l'université, 4460, Saint Nazaire cedex, France  
mouloud.feliachi@univ-nantes.fr, gerard.berthiau@univ-nantes.fr

<sup>3</sup>Laboratoire de génie électrique de Jijel (L2EI)  
Université de Jijel, 18000 Jijel, Algérie  
allag\_hic@yahoo.fr

<sup>4</sup>Department of Electrical Engineering, Hafr Al-Batin University, Hafr Al-Batin 31991, Saudi Arabia  
Boucekara.houssem@gmail.com

**Abstract** — In this work, the identification of the residual magnetic flux density of NdFeB permanent magnet, used in a drum magnetic separator, is performed. This identification problem has been formulated as an inverse optimization problem and solved using the Particle Swarm Optimization (PSO) method. For fast calculations, flux densities are computed using a 3D analytical method and the obtained results are compared with measurements.

**Index Terms** — 3D analytical solution, inverse problem, magnetic separation, parameters identification, Particle Swarm Optimization, permanent magnet.

### I. INTRODUCTION

In magnetic separation applications, the efficiency of the separation depends strongly upon the configuration of the applied magnetic field [1-4]. To design a reliable magnetic separator both the geometrical and magnetic specifications of the field generator must be accurately known.

The identification problem in physics devices is largely treated. In [5] the authors presented a simultaneous identification and control of adaptive torque of permanent magnet synchronous machines. In [6] a multiple object positioning and identification method based on the magnetic tracking system was proposed for tracking of minimally invasive medical devices inside human body, such as wireless capsule endoscope. In electrical machine domain, an inverse problem coupled with an analytical model was used for the identification of demagnetization

faults in axial flux permanent magnet synchronous machines [7]. Zhe et al. [8] proposed an identification procedure for an Active Magnetic Bearing System (AMBS), which makes it possible to estimate the unknown parameters and to establish the model of transfer function matrix of the AMB system.

The aim of this paper is the identification of the three components of the residual magnetic flux density  $\vec{B}_r(B_{rx}, B_{ry}, B_{rz})$  of an NdFeB permanent magnet constituting a rectangular bar with size  $1.2 \times 1 \times 10 \text{cm}^3$  used to realize a drum magnetic separator (see Fig. 1). For that, an inverse optimization problem is formulated and then solved where the objective function is the Mean Squared Error (MSE) between measured and computed values of the magnetic flux density in three different locations in the permanent magnet.

In the field of electromagnetics, several optimization methods have been used to solve different problems as reported in [9-17]. In this paper, the Particle Swarm Optimization (PSO) method has been used to solve the defined problem and the Most Valuable Player Algorithm (MVPA) is used for comparison purposes.

An experimental setup has been developed to measure the magnetic flux density of the permanent magnet. This last one has a parallelepiped shape and a rigid magnetization, this allows to use a 3D (in Cartesian coordinates) analytical integration method [18-19]. Such a solution is more accurate and faster than numerical ones which will make the optimization process faster.

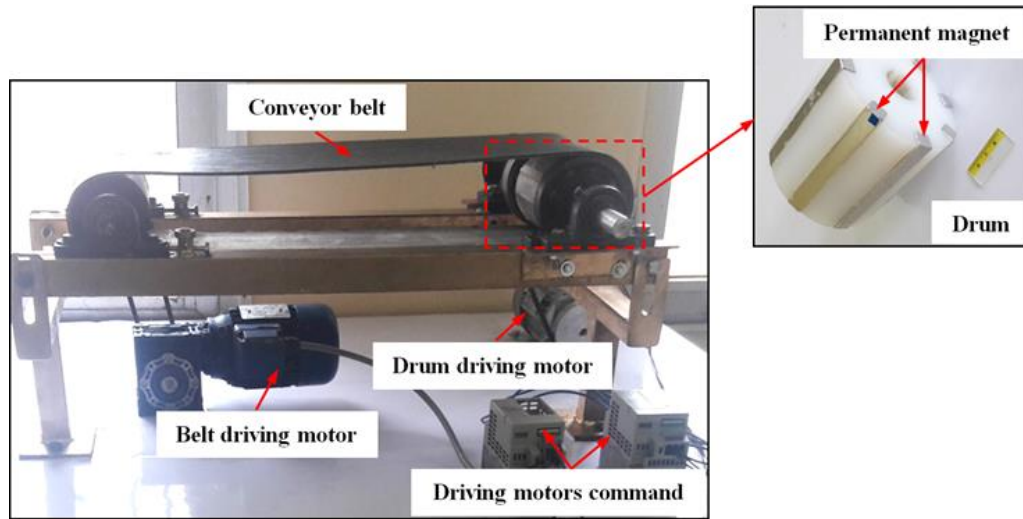


Fig. 1. Experimental setup of the magnetic drum separator.

## II. GENERATED MAGNETIC FIELD AND LOCATION OF MEASUREMENT FOR OPTIMIZATION

To know the accurate configuration of the magnetic field generated by the used permanent magnet, measurements have been performed. For this, we have realized and used the experimental test bench presented in Fig. 2.

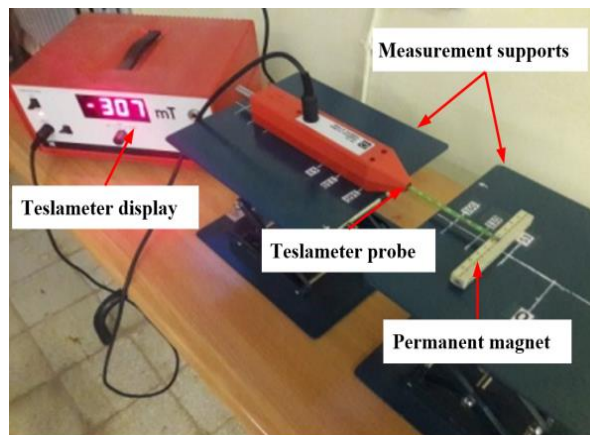


Fig. 2. Experimental setup for measuring the magnetic field.

To define the number of measuring locations required for the optimization process, we have measured and analyzed the magnetic flux density on all the faces of the permanent magnet. To show the nature of the variations of the magnetic flux density on the magnet

surfaces, we present the variation of the measured magnetic flux density along the length of two lines situated in significant surfaces oriented in the  $\vec{y}$  and  $\vec{z}$  directions (see Fig. 3). The line 2 is chosen near the corner of the permanent magnet because along the middle line of this surface the magnetic flux density ( $B_y$ ) is zero.

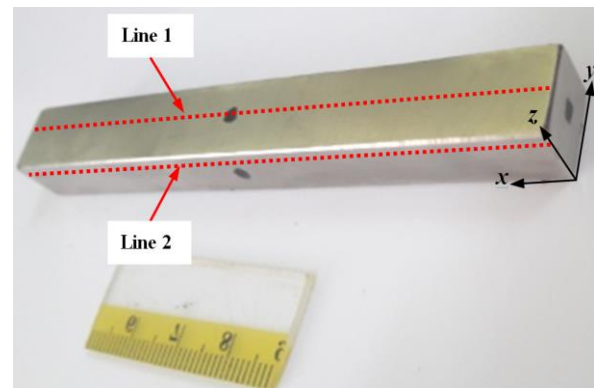


Fig. 3. Lines where the variation of the magnetic flux density is measured.

As shown in Fig. 4 (a), the magnetic flux density is almost constant along the length of the considered line of the significant surfaces of the permanent magnet except at the borders. Using this result along with the fact that each two opposite surfaces of the permanent magnet have opposite magnetic polarities, measuring locations for the optimization are reduced to only three locations located at the center of the three surfaces (see Fig. 4 (b)).

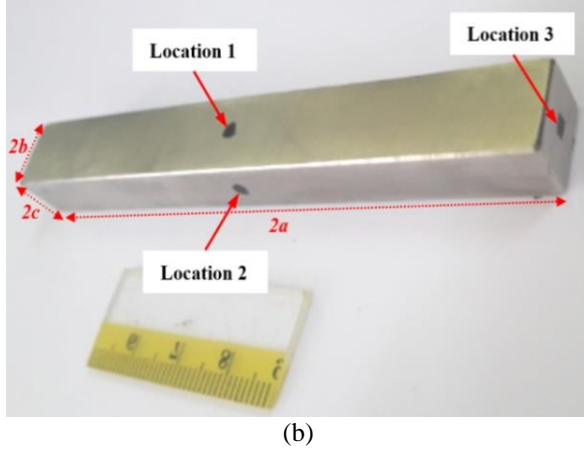
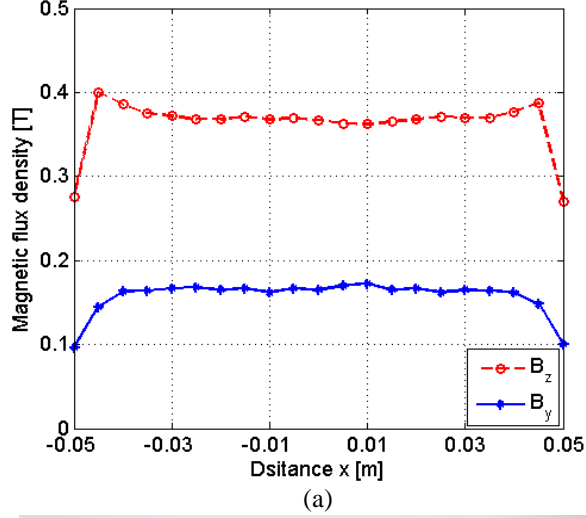


Fig. 4. (a) Variation of the magnetic flux density along the considered lines, and (b) the three measuring locations for the optimization process.

### III. PROBLEM FORMULATION

As aforesaid, the identification problem treated in this paper has been formulated as an inverse optimization problem where the design variables are the three components of the residual magnetic flux density  $B_{rx}$ ,  $B_{ry}$  and  $B_{rz}$  of the permanent magnet bar and the objective function is MSE between measured and computed values at three different locations. The objective function can be expressed as follows [20]:

$$F = \frac{1}{2} \sum_{i=1}^3 (B_{mi} - B_{ci})^2, \quad (1)$$

where  $B_{mi}$  and  $B_{ci}$  are respectively the measured and computed values at the locations  $i$  ( $i = 1, 2, 3$ ). In (1), the computed values  $B_{ci}$  are function of the three researched parameters  $B_{ci} = f(B_{rx}, B_{ry}, B_{rz})$ .

To compute the quantities  $B_{ci}$  we have used the 3D

analytical solution given by [21-22]:

$$\begin{bmatrix} B_x \\ B_y \\ B_z \end{bmatrix} = \frac{1}{4\pi} \sum_{i=0}^1 \sum_{j=0}^1 \sum_{k=0}^1 (-1)^{i+j+k} \begin{bmatrix} \operatorname{tg}^{-1}\left(\frac{VW}{rU}\right) & \ln(r-W) & \ln(r-V) \\ \ln(r-W) & \operatorname{tg}^{-1}\left(\frac{WU}{rV}\right) & \ln(r-U) \\ \ln(r-V) & \ln(r-U) & \operatorname{tg}^{-1}\left(\frac{UV}{rW}\right) \end{bmatrix} \begin{bmatrix} B_{rx} \\ B_{ry} \\ B_{rz} \end{bmatrix}. \quad (2)$$

The intermediary variables  $U$ ,  $V$  and  $W$  are given by [21-22]:

$$\begin{cases} U = x - (-1)^i a, & V = y - (-1)^j b, & W = z - (-1)^k c \\ r = \sqrt{U^2 + V^2 + W^2} \end{cases}. \quad (3)$$

The steps followed to obtain expression (2) are developed in the Appendix.

It is worth to mention that, the choice of three locations to measure the magnetic flux density (the perpendicular component at each face) has considerably reduced the computational time for the optimization process.

### IV. OPTIMIZATION METHOD AND OBTAINED RESULTS

To minimize the objective function, the PSO method has been applied [23]. It is a population-based stochastic algorithm and one of the global optimization methods, it simulates the migration and aggregation of animals, such as birds, fishes and bees when they seek for food. The basic form of the PSO algorithm is based on the evolution or movement of a population (called a swarm) of candidate solutions (called particles) in the search space. Each one of these particles has its position, velocity and a fitness value that is determined by an optimization function. The optimization is performed in terms of the objective function where each particle knows its best position obtained individually so far and is called the Personal Best ( $P_{pbest}$ ). In the same way, the other particles know what is the best position obtained collectively so far and is called the Global Best ( $P_{gbest}$ ). Each particle updates its velocity and position at each iteration by using the mathematical models given by [24].

$$v_m(t+1) = \omega v_m(t) + c_1 r_1 (P_{pbest}(t) - x_m(t)) + c_2 r_2 (P_{gbest}(t) - x_m(t)), \quad (4)$$

$$x_m(t+1) = x_m(t) + v_m(t+1), \quad (5)$$

where  $m$  is the particle number,  $v$  and  $x$  are the particle velocity and position, respectively,  $c_1$  is the cognitive coefficient,  $c_2$  is the social coefficient,  $r$  is a random values in the interval  $[0, 1]$  and  $\omega$  is the inertia weight who ensures that the particle swarm can search from the whole search space in the early iterations and converge in later iterations. The PSO method used in this paper is implemented according to the pseudo code given in Algorithm 1 [25].

**Algorithm 1: Pseudocode of the PSO method**

```

1  Input: Problem Size; Population Size
2  Output:  $P_{gbest}$ 
3  Population  $\leftarrow \emptyset$ 
4   $P_{gbest} \leftarrow \emptyset$ 
5  for  $i=1$ : population Size
6       $P_{velocity} \leftarrow$  Random Velocity
7       $P_{position} \leftarrow$  Random Position
8       $P_{pbest} \leftarrow P_{position}$ 
9      if  $\text{cost}(P_{pbest}) \leq \text{cost}(P_{gbest})$ 
10          $P_{gbest} \leftarrow P_{pbest}$ 
11      end
12  end
13  while (Stop condition)
14      for each  $P \in$  Population
15          $P_{velocity} \leftarrow$  Update
16         Velocity( $P_{velocity}, P_{gbest}, P_{pbest}$ )
17          $P_{position} \leftarrow$  Update
18         Position( $P_{position}, P_{velocity}$ )
19         if  $\text{cost}(P_{position}) \leq \text{cost}(P_{pbest})$ 
20              $P_{pbest} \leftarrow P_{position}$ 
21         if  $\text{cost}(P_{pbest}) \leq \text{cost}(P_{gbest})$ 
22              $P_{gbest} \leftarrow P_{pbest}$ 
23         end
24     end
25  end
26  return  $P_{gbest}$ 

```

In this paper, the PSO method has been programmed using the commercial MATLAB software and run on a computer with Intel(R) Xeon(R) CPU E5-1620 v2 @ 3.70 GHz Processor and 8.00 GO-RAM under professional windows 7 environment. The stopping criterion was chosen as  $\varepsilon = 1 \times 10^{-9}$  so that the iteration stopped when  $F \leq \varepsilon$ . The tuning parameters used for the PSO algorithm are listed in Table 1.

Table 1: PSO tuning parameters

Parameters	Values
Population Size	40
Cognitive coefficient $c_1$	-0.6504
Social coefficient both $c_2$	2.2073
Inertia weight $\omega$	-0.4349
Range of the researched parameters	[-1.3 1.3]

The optimal design variables found after 27 iterations are displayed in Table 2.

Table 2: Optimal values found after 27 iterations

Parameters	Values
$B_{rx}(T)$	$-2.27 \times 10^{-5}$
$B_{ry}(T)$	$1.39 \times 10^{-5}$
$B_{rz}(T)$	1.1066
$F$	$1.94 \times 10^{-10}$
$t(s)$	0.1989

The results of Table 2 show that the dominant component of the residual flux density is  $B_{rz}$  which signifies that the magnetization of the permanent magnet is oriented in the z-axis direction. To verify the obtained results, we have computed the magnetic flux density along the lines of Fig. 3. The comparison between the computed and measured values is presented in Fig. 5.

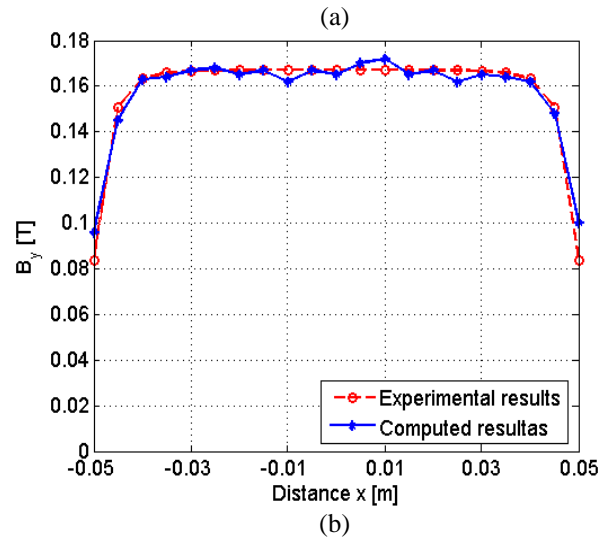
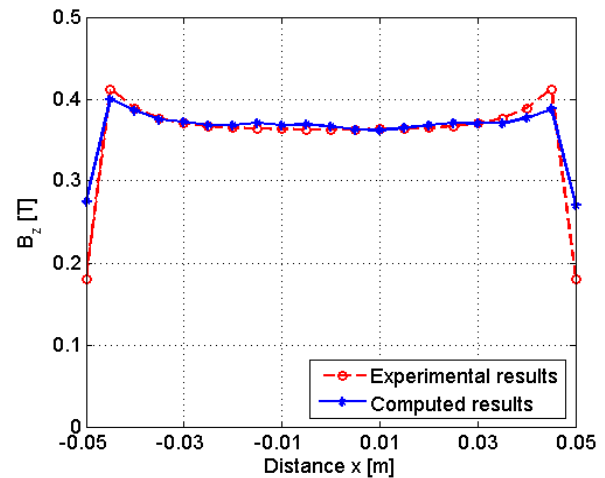


Fig. 5. Variation of the magnetic flux density related to the identified parameters. (a) Variation along the length of the line 1, and (b) variation along the length of the line 2.

Figure 5 shows that the measured and computed results are very close, which validates the reliability of the developed computing codes and the obtained results.

For a global verification of the achieved optimization, we have compared the results obtained by the PSO with those obtained by the Multi Valuable Player Algorithm (MVPA) method.

The MVPA is a recently developed algorithm inspired from sport [16]. It is a very competitive algorithm compared with other optimization algorithms as proved in [26] and [27]. The pseudo code of the MVPA is given in Algorithm 2 and the main steps are detailed bellow. Like other population-based metaheuristics, the MVPA starts by generating a population of players inside the search space following a random distribution. These players are regrouped into teams (line 3). Then the algorithm will iterate 'MaxNFix' times trying to evolve the population to find the optimal solution. In each iteration, a loop on all teams selects a first team called TEAM<sub>i</sub>. The players of this team compete to determine to best player (Franchise Player) of this team and the population is updated accordingly (line 8). This first phase is called the 'individual competition phase'. In the second competition phases called 'team competition phase', a second team called TEAM<sub>j</sub> is randomly selected among the leagues' teams. TEAM<sub>i</sub> and TEAM<sub>j</sub> play against each other to determine the wining team. The population is updated according to the outcome of this matchup (lines 9-13). Once the competition phase is completed the players are checked to see if there is any player outside the search space. In such case, this player is brought back to the search space (line 14). In order to improve the performance of the MVPA three steps have to be performed which are 'application of greediness', 'application of elitism' and 'remove duplicates'. In the first step, a player is updated only if his new fitness is better than the old one. In the second step, some of the worst players are replaced by some of the best players. In the third step duplicate players are removed and changed by new ones.

In the pseudocode of the MVPA, the inputs are the function (ObjFunction), the number of design variables (ProblmSize), the number of players which is equivalent to the population size (PlayersSize), the number of teams in the league (TeamsSize) and the maximum number of fixtures which is equivalent to the maximum number of iterations (MaxNfix). The output of the algorithm is the league's MVP which is the best solution obtained.

To estimate the speed of convergence of the two applied methods, Fig. 6 plots the evolution of the objective function versus the number of iterations.

#### Algorithm 2: Pseudocode of the MVPA method

**Inputs:** ObjFunction (objective function), ProblemSize (dimension of the problem), PlayersSize (number of players), TeamsSize (number of teams) and MaxNFix (maximum number of fixtures)

**Output:** MVP

1 Initialization

2 **for** fixture=1:MaxNFix

3     **for** i=1:TeamsSize

4         TEAM<sub>i</sub> =Select the team number i from the league's teams

5         TEAM<sub>j</sub> = Randomly select another team j from the league's teams where j≠i

6         TEAM<sub>i</sub> = TEAM<sub>i</sub> + rand × (FranchisePlayer<sub>i</sub> – TEAM<sub>i</sub>) + 2 × rand × (MVP – TEAM<sub>i</sub>)

7         **if** TEAM<sub>i</sub> wins against TEAM<sub>j</sub>

8             TEAM<sub>i</sub> = TEAM<sub>i</sub> + rand × (TEAM<sub>i</sub> – FranchisePlayer<sub>j</sub>)

9         **else**

10             TEAM<sub>i</sub> = TEAM<sub>i</sub> + rand × (FranchisePlayer<sub>j</sub> – TEAM<sub>i</sub>)

11         **end**

12     Check if there are players outside the search space

13     **end**

14     Application of greediness

15     Application of elitism

16     Remove duplicates

17 **end for**

A comparison between the results obtained by PSO and those obtained by MVPA method is shown in Table 3.

Table 3: Optimal values of the researched parameters obtained by the two methods

Parameters	PSO	MVPA
$B_{rx}$ (T)	$-2.27 \times 10^{-5}$	$-1.07 \times 10^{-4}$
$B_{ry}$ (T)	$1.39 \times 10^{-5}$	$-1.34 \times 10^{-4}$
$B_{rz}$ (T)	1.1066	1.1069
$F$	$1.94 \times 10^{-10}$	$7.67 \times 10^{-10}$
$t$ (s)	0.1989	0.2505
Iteration's number	27	15

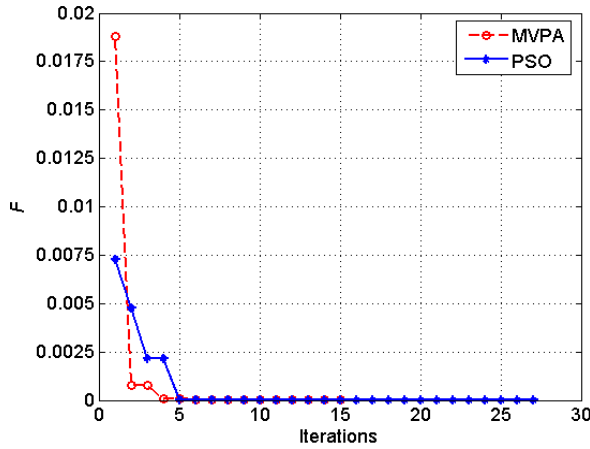


Fig. 6. Evolutions of the objective function as a function of computing iterations.

The comparison between the obtained results of the Table 3 and Fig. 6 show that the two applied optimization methods have given the same values of the three researched parameters corresponding to the three components of the residual magnetic flux density.

The obtained results show clearly that the MVPA converges quickly but the PSO algorithm performs better in terms of running time.

## V. CONCLUSION

In this work, developed for a magnetic separation study, a methodology for NdFeB permanent magnet parameters identification based on the resolution of an inverse problem has been presented. In such methodology, the PSO method is combined with 3D analytical solution, which has given a good accuracy and a low processing cost. The results of the analytical solution have been validated by comparison with measurements. For a global verification of the achieved optimization, we have compared the obtained results by the PSO with those obtained by the Multi Valuable Player Algorithm (MVPA) method. The comparison shows that the two applied methods have given the same optimal results. However, the PSO method presents better performances in terms of running time.

## ACKNOWLEDGMENT

This work was supported by the Inductics-Net of the ATRST agency and the DGRSDT Direction, Algerian section.

## APPENDIX

### Analytical calculation of magnetic flux density created by a magnet

Based on the conventional equivalent magnetic charge method, for parallel uniform magnetized magnet in  $z$  direction, the magnetization effect can be represented

by two parallel magnetic charge surfaces (Colombian approach) on the sides of the permanent magnet which their normal is collinear with the supposed magnetization direction [28].

An assumed rigid and uniform magnetization can be replaced by a distribution of magnetic poles. The density of such poles distribution is defined by [29]:

$$\sigma = \vec{M} \cdot \vec{n} = \frac{\vec{B}_r}{\mu_0} \cdot \vec{n}. \quad (6)$$

Let us consider the rectangular surface  $2a \times 2b$  having a uniform pole density  $\sigma$  (Fig. 7).

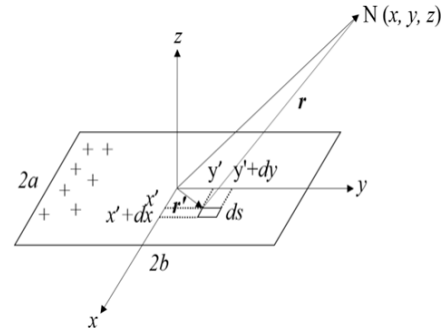


Fig. 7. Geometrical illustration for the potential and the magnetic field calculation.

The magnetic scalar potential  $V$  in a point  $N$  is given by [21-22]:

$$V = \frac{1}{4\pi} \iint_s \frac{M \cdot ds}{\|\vec{r} - \vec{r}'\|}. \quad (7)$$

Depending on the residual magnetic flux density, the expression (7) can be written as:

$$V = \frac{1}{4\pi\mu_0} \iint_s \frac{B_r \cdot ds}{\|\vec{r} - \vec{r}'\|}. \quad (8)$$

In Cartesian coordinates system, (8) can be written as:

$$V = \frac{B_r}{4\pi\mu_0} \int_{-b}^b dy' \int_{-a}^a \frac{1}{\sqrt{(x'-x)^2 + (y'-y)^2 + z^2}} dx'. \quad (9)$$

After two analytical integrations, we obtain:

$$V = \frac{B_r}{4\pi\mu_0} \sum_{i=0}^1 \sum_{j=0}^1 (-1)^{i+j} \left( -U \ln(r-V) - V \ln(r-U) - W \operatorname{tg}^{-1} \left( \frac{UV}{rW} \right) \right), \quad (10)$$

$$\begin{cases} U = x - (-1)^i a, & V = y - (-1)^j b, & W = z \\ r = \sqrt{U^2 + V^2 + W^2} \end{cases}. \quad (11)$$

The magnetic field can be calculated by deriving the scalar potential expression, which leads to:

$$\vec{H} = \frac{B_r}{4\pi\mu_0} \sum_{i=0}^1 \sum_{j=0}^1 (-1)^{i+j} \begin{pmatrix} \ln(r-V) \\ \ln(r-U) \\ \operatorname{tg}^{-1} \left( \frac{UV}{rW} \right) \end{pmatrix}. \quad (12)$$

So, the magnetic flux density is given by:

$$\vec{B} = \frac{B_r}{4\pi} \sum_{i=0}^1 \sum_{j=0}^1 (-1)^{i+j} \begin{pmatrix} \ln(r-V) \\ \ln(r-U) \\ \operatorname{tg}^{-1}\left(\frac{UV}{Wr}\right) \end{pmatrix}. \quad (13)$$

For a cubical magnet in which the magnetization is collinear with  $z$  direction, (see Fig. 8), the magnetic flux density can be determined from the upper and the lower charged surfaces.

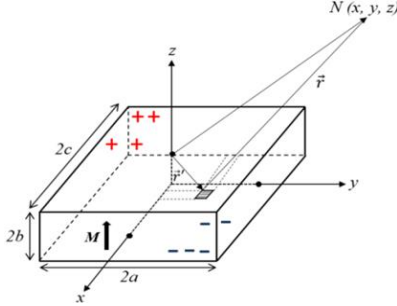


Fig. 8. Magnetic field created by a cuboidal permanent magnet.

In this case, comparing also to (equation 13), the magnetic flux density will be:

$$\vec{B} = \frac{B_r}{4\pi} \sum_{i=0}^1 \sum_{j=0}^1 \sum_{k=0}^1 (-1)^{i+j+k} \begin{pmatrix} \ln(r-V) \\ \ln(r-U) \\ \operatorname{tg}^{-1}\left(\frac{UV}{Wr}\right) \end{pmatrix}. \quad (14)$$

The intermediary variables become:

$$\begin{cases} U = x - (-1)^i a, V = y - (-1)^j b, W = z - (-1)^k c \\ r = \sqrt{U^2 + V^2 + W^2} \end{cases}. \quad (15)$$

For a permanent magnet magnetization oriented randomly in space, the global magnetization is the superposition of the three components as shown in Fig. 9:

$$\vec{M} = M_x \vec{i} + M_y \vec{j} + M_z \vec{k}. \quad (16)$$

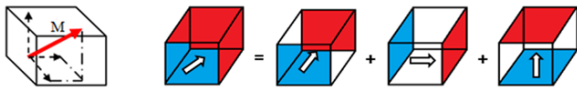


Fig. 9. Decomposition of a randomly oriented magnetization in a permanent magnet [22].

Then, the computation of the total components of is deduced as follows:

$$\vec{B} = \vec{B}_x + \vec{B}_y + \vec{B}_z, \quad (17)$$

According to the result given by  $z$  axis-oriented magnetization (7 to 13), the total  $B$  resulting from the inclined magnetization is given by a simple permutation of analytic formulas for the two other directions of magnetization ( $x$  axis and  $y$  axis). So, we can write:

$$\vec{B} = \frac{1}{4\pi} \sum_{i=0}^1 \sum_{j=0}^1 \sum_{k=0}^1 (-1)^{i+j+k} \begin{pmatrix} B_{rx} \operatorname{tg}^{-1}\left(\frac{WV}{rU}\right) + B_{ry} \ln(r-W) + B_{rz} \ln(r-V) \\ B_{rx} \ln(r-W) + B_{ry} \operatorname{tg}^{-1}\left(\frac{WU}{rV}\right) + B_{rz} \ln(r-U) \\ B_{rx} \ln(r-V) + B_{ry} \ln(r-U) + B_{rz} \operatorname{tg}^{-1}\left(\frac{VU}{rW}\right) \end{pmatrix}, \quad (18)$$

In other manner, we can write the magnetic flux density components as:

$$\begin{bmatrix} B_x \\ B_y \\ B_z \end{bmatrix} = \frac{1}{4\pi} \sum_{i=0}^1 \sum_{j=0}^1 \sum_{k=0}^1 (-1)^{i+j+k} \begin{bmatrix} \operatorname{tg}^{-1}\left(\frac{VW}{rU}\right) & \ln(r-W) & \ln(r-V) \\ \ln(r-W) & \operatorname{tg}^{-1}\left(\frac{WU}{rV}\right) & \ln(r-U) \\ \ln(r-V) & \ln(r-U) & \operatorname{tg}^{-1}\left(\frac{UV}{rW}\right) \end{bmatrix} \begin{bmatrix} B_{rx} \\ B_{ry} \\ B_{rz} \end{bmatrix}. \quad (19)$$

## REFERENCES

- [1] X. Zheng, N. Guo, R. Cui, et al., "Magnetic field simulation and experimental tests of special cross-sectional shape matrices for high gradient magnetic separation," *IEEE Transactions on Magnetics*, vol. 53, no 3, pp. 1-10, 2017.
- [2] R. Mehasni, M. E. H. Latreche, and M. Feliachi, "Effect of the magnetic dipole-dipole interaction on the capture efficiency in open gradient magnetic separation," *IEEE Trans on Magnetics*, vol. 43, no. 8, Aug. 2007.
- [3] A. Belounis, R. Mehasni, M. Ouili, and M. E. H. Latreche, "Optimization of the capture element for an OGMS based on the 3d computation of the magnetic particle behavior," *International Journal of Electromagnetic and Mechanics*, vol. 48, no. 4, pp. 387-397, 2015.
- [4] F. Mishima, Y. Akiyama, and S. Nishijima, "Fundamental study on magnetic separator using oxygen dissolved perfluorocarbon," *IEEE Transactions on Applied Superconductivity*, vol. 24, no. 3, pp. 1-5, 2014.
- [5] D. M. Reed, S. Jingand, and H. F. Hofmann, "Simultaneous identification and adaptive torque control of permanent magnet synchronous machines," *IEEE Transactions on Control Systems Technology*, vol. 25, no. 4, pp. 1372-1383, 2017.
- [6] S. Song, C. Hu, and M. Q. Meng, "Multiple objects positioning and identification method based on magnetic localization system," *IEEE Transactions on Magnetics*, vol. 52, Oct. 2016.
- [7] J. De Bisschop, A. Abdallah, P. Sergeant, and L. Dupré, "Identification of demagnetization faults in axial flux permanent magnet synchronous machines using an inverse problem coupled with

- an analytical model,” *IEEE Transactions on Magnetics*, vol. 50, no. 11, Nov. 2014.
- [8] S. Zhe, H. Ying, Z. Jingjing, S. Zhengang, Z. Lei, and Y. Suyuan, “Identification of active magnetic bearing system with a flexible rotor,” *Elsivier, Mechanical Systems And Signal Processing*, vol. 49, no. 2, pp. 302-316, Dec. 2014.
- [9] H. Boudjefdjouf, H. R. H. Bouchekara, F. de Paulis, et al., “Wire fault diagnosis based on time-domain reflectometry and backtracking search optimization algorithm,” *Applied Computational Electromagnetics Society Journal*, vol. 31, no. 4, 2016.
- [10] J. Pzolghadr, Y. Cai, and N. Ojaroudi, “UWB slot antenna with band-notched property with time domain modelling based on genetic algorithm optimization,” *Applied Computational Electromagnetics Society Journal*, vol. 31, no. 8, 2016.
- [11] R. Carlos, K. Tine, and G. Alejandro, “Identification of a proton-exchange membrane fuel cell’s model parameters by means of an evolution strategy,” *IEEE Transactions on Industrial Informatics*, vol. 11, no. 2, July 2014.
- [12] S.-Y. Kuo and Y.-H. Chou, “Entanglement-enhanced quantum-inspired Tabu search algorithm for function optimization,” *IEEE Access*, vol. 5, pp. 13236-13252, 2017.
- [13] F. Campelo, F. G. Guimarães, H. Igarashi, J. A. Ramirez, and S. Noguchi, “A modified immune network algorithm for multimodal electromagnetic problems,” *IEEE Transactions on Magnetics*, vol. 42, no. 4, pp. 1111-1114, Apr. 2006.
- [14] F.-P. Xiang, E.-P. Li, X.-C. Wei, and J.-M. Jin, “A particle swarm optimization-based approach for predicting maximum radiated emission from PCBs with dominant radiators,” *IEEE Trans on Electromagnetic Compatibility*, vol. 57, pp. 1197-1205, 2015.
- [15] L. D. S. Coelho, L. D. Afonso, and P. Alotto, “A modified imperialist competitive algorithm for optimization in electromagnetics,” *IEEE Transactions on Magnetics*, vol. 48, no. 2, pp. 579-582, 2012.
- [16] H. R. E. H. Bouchekara, “Most valuable player algorithm: A novel optimization algorithm inspired from sport,” *Operational Research*, pp. 1-57, May 10, 2017.
- [17] H. R. H. Bouchekara, M. Nahas, and H. M. Kaouach, “Optimal design of electromagnetic devices using the league championship algorithm,” *Applied Computational Electromagnetics Society Journal*, vol. 32, no. 6, 2017.
- [18] A. Azzouza, H. Allag, J.-P. Yonnet, and P. Tixador, “3-D new calculation principle of levitation force between permanent magnet and hard type-II superconductor using integral approach,” *IEEE Trans. Magn.*, vol. 53, no. 11, 2017.
- [19] H. Allag, J.-P. Yonnet, H. R. H. Bouchekara, et al., “Coulombian model for 3d analytical calculation of the torque exerted on cuboidal permanent magnets with arbitrary oriented polarizations,” *Applied Computational Electromagnetics Society Journal*, vol. 30, no. 4, 2015.
- [20] M. Hadeif, M. R. Mekideche, and H. Allag, “Relative magnetic permeability identification of the permanent magnets of a synchronous motor using inverse problem,” *International Review of Electrical Engineering (IREE)*, vol. 2, no. 2, pp. 103-109, 2007.
- [21] A. Gilles and J.-P. Yonnet, “3D analytical calculation of the forces exerted between two cuboidal magnets,” *IEEE Trans on Magnetics*, vol. mag-20, no. 5, Sep. 1984.
- [22] H. Allag, J.-P. Yonnet, and M. E. H. Latreche, “3D analytical calculation of forces between linear Halbach-type permanent magnet arrays,” *8th International Symposium on IEEE*, pp. 1-6, 2009.
- [23] J.-H. Lee, J.-W. Kim, J.-Y. Song, et al., “Distance-based intelligent particle swarm optimization for optimal design of permanent magnet synchronous machine,” *IEEE Trans on Magnetics*, vol. 53, no. 6, 2017.
- [24] C. Zhang, Z. Chen, Q. Mei, et al., “Application of particle swarm optimization combined with response surface methodology to transverse flux permanent magnet motor optimization,” *IEEE Trans on Magnetics*, vol. 53, no. 12, pp. 1-7, 2017.
- [25] J. Brownlee, “Clever algorithms: nature-inspired programming recipes,” *Jason Brownlee*, 2011.
- [26] B. Alatas, “Sports inspired computational intelligence algorithms for global optimization,” *Artificial Intelligence. Rev.*, 2017.
- [27] H. R. E. Bouchekara, A. Orlandi, M. Al-Qdah, and F. de Paulis, “Most valuable player algorithm for circular antenna arrays optimization to maximum sidelobe levels reduction,” *IEEE Transactions on Electromagnetic Compatibility*, vol. 60, no. 6, 2018.
- [28] H. Zhang, B. Kouet, and L. Li, “Analytical calculation of the 3D magnetic field created by non-periodic permanent magnet arrays,” in *Electrical Machines and Systems (ICEMS) 2011 International Conference on IEEE*, pp. 1-4, 2011.
- [29] F. J. Maarten, J. J. H. Paulides, and E. Ilhan, “Relative permeability in a 3d analytical surface charge model of permanent magnets,” *IEEE Trans. on Magnetics*, vol. 49, no. 5, May 2013.





**Mehdi Ouili** was born in Constantine, Algeria, in 1987. He received the B.S. and M.S. degrees in Electrical Engineering from the University of Constantine, Algeria in 2010 and 2013 respectively. He is currently working toward the Ph.D. degree at the Department of Electrical Engineering, in the same University, member of the LEC laboratory. His current research interests include magnetic separation process.



**Rabia Mehasni** was born in Grarem, Algeria, in 1970. He received the Ph.D. in Electrical Engineering from the University of Constantine, Algeria in 2007. He is with the Department of Electrical Engineering, University of Constantine since 2000. He is currently Research Director at the LEC Laboratory. He has published in the field of magnetic separation. His research interests are in the field of numerical methods and modeling techniques to approach the multidisciplinary problems.



**Mouloud Feliachi** is native of Biskra in Algeria. He is an Engineer of the “Ecole Nationale Polytechnique” of Algiers (1976), a Ph.D. of the “Conservatoire National des Arts et Métiers” of Paris (1981) and “Docteur d'Etat Es-Sciences Physiques” of the “Institut National Polytechnique” of Grenoble (1986), all in Electrical Engineering. In 1987, he worked as an Engineer for the Leroy Somer company in Orléans. In 1988, he joined the University of Nantes (Institut Universitaire de Technologie - Saint-Nazaire) where he is Professor. He was Scientific Director of LRTI-Lab and Head of the Modeling and Simulation team in GE44-Lab. He is currently leading a Franch-Algerian thematic network of research in Inductics, within IREENA Lab. His research interests are in hybrid analytical and numerical modeling of low frequency electromagnetic phenomena with emphasis on multiphysics and eddy current non-destructive testing and evaluation.



**Hichem Allag** received the diploma of Engineer in Electrical Engineering from the University of Jijel (Algeria) and the magister from University of Constantine in respectively 2000 and 2002. He was qualified as Assistant Professor in Jijel University in 2003. From 2007 to 2010, he prepared and received the Ph.D. in the

University of Joseph Fourier in France. He is currently Professor in University of Jijel, Director of Electro-technic and Industrial Electronic Laboratory, Head of Department of Fundamental Sciences and Technology. His scientific researches include computational electromagnetic and control applications.



**Housseem R.E.H. Bouchekara** is an Associate Professor at the Electrical Engineering Department of University of Hafr Al Batin. He has received his B.S. in Electrical Engineering from University Mentouri Constantine, Algeria, in 2004. He has received his Master in Electronic Systems and Electrical Engineering from Polytechnic School of the University of Nantes, France, 2005. He received his Ph.D. in Electrical Engineering from Grenoble Institute of Technology, France, in 2008. His research interest includes: optimization techniques, magnetic refrigeration, electromagnetics, electric machines and Power systems.



**Gerard Berthiau** received the M.S. and Engineer degrees in Scientific Computing from Conservatoire National des Arts et Métiers in 1991, Ph.D. degree in Electronics from Ecole Centrale Paris in 1994 and the “Habilitation à Diriger les Recherches” at the University of Nantes in 2007. He is currently a Full Professor in the Department of Physics at the Institute of Technology of Saint-Nazaire, Nantes University, France. His current research interests include electromagnetic field computation and physical properties characterization for non destructive testing particularly for composite materials, inverse problems and optimization techniques.



**Mohamed El Hadi Latreche** is a Professor in the Electrical Engineering Department of the University Mentouri of Constantine, in Algeria. He is a researcher in LEC Laboratory of Constantine and his research area is the electromagnetic field and numerical calculations, with a focus on electromagnetic induction phenomena, and optimization structures. He has published more than 20 academic articles and participated in more than 50 scientific conferences.